JOURNAL OF MATERIALS SCIENCE 35 (2000) 5407–5413

Effect of a cerium/tin doping mixture on the texturing process and on the superconducting properties of top seeded melt textured YBaCuO

C. LEBLOND-HARNOIS*, I. MONOT, G. DESGARDIN
Laboratoire CRISMAT, UMR CNRS 6508, ISMRA, 6 Bd Marechal Juin 14050 CAEN cedex, France
E-mail: christelle.leblond@ismra.fr

The influence of a cerium/tin doping mixture on top seeded melt textured pellets of $YBa_2Cu_3O_{7-\delta}/Y_2BaCuO_5$ (Y123/Y211) was investigated and compared with cerium doping. The thermal cycle of the texturing process has been adapted to this new composition, considering the variations of the decomposition temperature and of the melt viscosity. Growth rates of YBCO crystals appear to be quadrupled by the presence of tin. We manage to grow domains of diameter 30 mm from a $SmBa_2Cu_3O_{6+\delta}$ seed. SEM observations have shown no modification of the Y_2BaCuO_5 inclusions either in size or in morphology compared to Y211 particules in cerium doped YBCO. However, EDS analyses have revealed the existence of submicron particles containing Y, Ba, Cu, Sn, Ce and O distributed in the matrix. Superconducting properties are greatly improved by the addition of a moderate amount of tin to the cerium doped YBCO. The critical temperature is shifted toward 92 K with a transition width of 0.5 K. Critical current densities at 77 K reach values as high as 9×10^4 A/cm^2 in self field, 5×10^4 A/cm^2 under 1 Tesla and still 2.5×10^4 A/cm^2 under 2 T, which are among the best results ever obtained for top seeded doped YBCO.

1. Introduction

Applications of YBCO bulk material as levitated trains [1, 2], flywheel energy storage systems [3, 4] or contactless superconducting bearings [5] require the obtention of large, oriented pellets with high critical current densities (J_c). Pellets as large as 10 cm have already been successfully textured by the top seeding melt texturing process [6], which is the most commonly used method to texture large monoliths of REBaCuO material. Numerous attempts have been carried out to improve the current density by the addition of different dopants, more or less effective, such as SiC, $BaZrO_3$ [7], Pt [8–10], $BaSnO_3$ or SnO_2 [7, 11–15] or CeO_2 [16–19]. These latter two compounds have been widely studied and present great interest for the texturing process and the superconducting properties. The SnO_2 addition, decreasing the melt viscosity, results in an increase of the Y diffusion in the melt and thus, of the growth rate of YBCO. Moreover, the very fine (micron to submicron) Sn rich inclusions trapped in the matrix act as flux pinning centres and lead to higher current densities in low fields [20, 21].

CeO_2 doping inhibits the Y_2BaCuO_5 (Y211) coarsening in the melt and thus yields higher values of J_c at low fields. On the other hand, CeO_2 has been shown to increase the melt viscosity, which decreases the growth rate of the textured domains.

As a result, it is interesting to study a combination of these two dopants. Such a study has recently been started by Marinel *et al*. [21] on microwave melt textured YBCO bars. The authors have found an increase of the growth rates and an improvement of superconducting properties. Their work reveals the possible existence of an optimum in the SnO_2 content for a fixed CeO_2 content.

This article deals with the effects of the $CeO_2 + SnO_2$ doping combination on the texturing process and on superconducting properties of YBCO top seeded pellets, compared with CeO_2 only doping. We report the adaptation of texture cycles to this new composition and the microstucture of the materials obtained. Zero field cooled levitation forces, critical temperatures and current densities have also been measured.

2. Experimental details

Raw powders of commercial $YBa_2Cu_3O_{7-\delta}$ (Y123) (Solvay Barium Strontium) and commercial spray dried Y211 (Seattle Specialty Ceramics) were used. The doping compounds have a purity of 99.9 % for

* Author to whom all correspondence should be addressed.

CeO_2 (Aldrich) and 99 % for SnO_2 (Prolabo). Three compositions have been studied:

A : Y123 + 0.25 mole Y211(called $Y_{1.5}$)
+ 0.5 wt % CeO_2,

B : Y123 + 0.25 mole Y211 + 0.5 wt % CeO_2
+ 0.25 wt % SnO_2 (i.e.1 mole % SnO_2) and

C : Y123 + 0.25 mole Y211 + 0.5 wt % CeO_2
+ 1 wt % SnO_2 (i.e.4 mole % SnO_2).

The Y211 and CeO_2 contents had already been optimised in a previous study for composition A [19], and only the influence of the SnO_2 content was studied here. 30 mm diameter pellets of each composition were uniaxially pressed at 1 t/cm^2. A seed of melt grown $SmBa_2Cu_3O_{7-\delta}$ was placed on the pellets before the texturing step. Seeds orientation and quality were checked by Lauë diffraction. The process followed to obtain large monoliths in the case of cerium doping is described in detail in [19]. Briefly, a "pre-sintering" step at 1000°C is applied to the pressed pellets in order to decarbonate the material and homogenise their composition. The samples are subsequently decomposed at 1045°C during 5 hours before the cooling down. The cooling rate is reduced inside the nucleation window. This temperature window is delimited by the temperatures of heterogeneous nucleation of Y123 from the seed and of homogeneous nucleation in the melt. The cooling rate is adjusted to yield the desired final domain size from the knowledge of the Y123 growth rates inside the temperature window. For composition A, the nucleation window was determined to be 990°C–980°C. The composition A sample, used as reference in this study, has a textured top surface of 2.2 × 2.2 cm^2. These dimensions remain unchanged for the whole domain depth. The textured thickness is 1 cm with the texture quality equivalent to that described in [19]. The same process was applied for the other compositions except the specific texturing cycle temperatures. Textured pellets were subsequently annealed for 150 hours at 430°C under oxygen flow.

Decomposition temperatures were determined by differential thermal analysis (DTA) using Setaram apparatus (labsys). The curves were recorded using a heating rate of 2°/min. Micrographs were taken on polished surfaces with a scanning electron microscope (SEM, FEG XL 30 Philips). The levitation forces were obtained using the system described in [19]. The forces were measured in zero field cooled with a SmCo magnet of 25 mm diameter ($B_s = 0.40$ T). Superconducting properties were measured on cleaved samples (typically 2 × 2 mm^2) using a SQUID magnometer at 77 K with the field applied parallel to the sample *c* axis. The critical current densities were calculated using the modified Bean model [22] from the magnetisation curves.

3. Results

3.1. Texturing process

The texturing of pellets of composition A is well controlled and single domains of more than 30 mm diameter are now obtained routinely [19, 23]. To adapt the thermal cycle optimised for cerium doped samples to the Ce + Sn doped samples, decomposition temperatures of the different compositions were determined by DTA. Fig. 1a shows the DTA curves for the various compositions. The first peak, referred as (1) on the figure, corresponds to a decarbonation step and is present for all the compositions. The second peak marks the decomposition temperature. Table I gives the values measured. For information, we precise that $Y_{1.5}$ + 0.25 wt % SnO_2, and with no cerium, has also been measured and presents the same temperature values as undoped $Y_{1.5}$. It appears that cerium reduces the decomposition temperature by approximatively 20 degrees. On the contrary, the addition of SnO_2 to the cerium doped material, whatever the tin content,

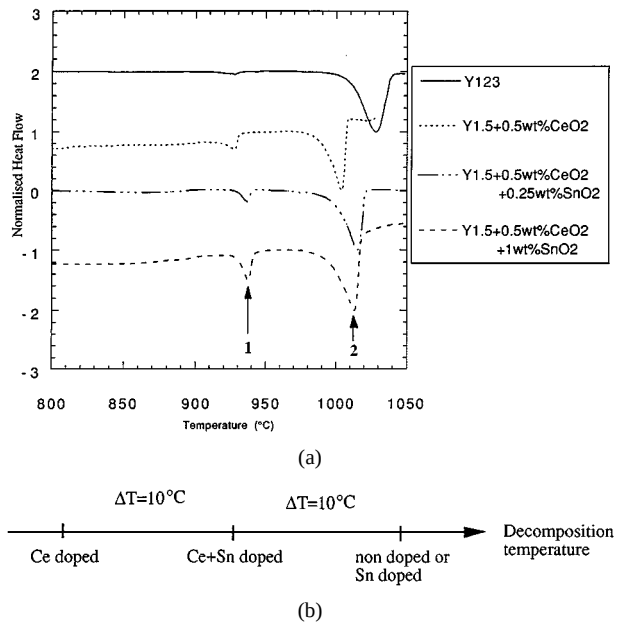

Figure 1 (a) DTA curves obtained for the different compositions. Peak referred as (1) corresponds to a decarbonation step. Peak referred as (2) marks the decomposition temperature of Y123; (b) Schematic illustrating the differences in the decomposition temperatures versus the doping element.

TABLE I Decarbonation and decomposition temperatures measured on the DTA curves versus composition

	$Y_{1.5}$	$Y_{1.5}$ +0.5 wt % CeO_2	$Y_{1.5}$ +0.5 wt % CeO_2 +0.25 wt % SnO_2	$Y_{1.5}$ +0.5 wt % CeO_2 +1.0 wt % SnO_2
$T_{decarbonatation}$	927°C	928°C	936°C	937°C
$T_{decomposition}$	1028°C	1004°C	1015°C	1013°C

increases this temperature by 10 degrees. These results are summarised schematically in Fig. 1b.

By comparison, the maximum temperature for Ce + Sn doping was therefore chosen to be 10 degrees more than for Ce only doping, i.e. 1055°C. Attempts to texture samples have resulted in the formation of deformed pellets, with significant liquid losses, suggesting that 1055°C is too high. This could be easily explained by the fact that SnO_2 is well known to reduce the melt viscosity, unlike CeO_2. Thus, the maximum temperature should be a compromise between the viscosity and the decomposition temperature of the mixture. The final choice was then 1050°C.

The nucleation window was determined from several quench experiments following 5 hours at 1050°C. The temperature of nucleation from the seed was found to be 986°C and homogeneous nucleation in the melt appears at 981°C. Growth rates calculated from the progress of the growth fronts between 986°C and 981°C are 1.55 mm/h in the *ab* planes and 1.8 mm/h along the *c* direction. In the case of cerium doping, the values were found to be 0.4 mm/h in the *ab* planes and 0.25 mm/h along *c* [19]. It is clear that tin enhances the growth rates significantly.

Taking into account all these parameters, a new texturing cycle was defined for Ce + Sn doped samples. No "pre-sintering" step was applied for this first study. Indeed, since the melt is more fluid, it was assumed that CO_2 and O_2 gas would escape more easily from the pellets and, secondly, homogeneity of the pellets would be favoured. The thermal cycle is shown in Fig. 2. By this process, 30 mm diameter pellets of composition B were successfully textured as illustrated in Fig. 3. Apparent domain surface is 2.5×2.5 cm^2. Homogeneous nucleation in the melt is however significant at the sides of the pellet.

On the other hand, the growth of single domains of composition C failed. All the attempts lead to the formation of small multidomains at the seed position (less than 0.5 cm^2 surface). Remark that no doubt can fall on initial seeds quality as they were selected with special care. After the texturing process, seeds have a porous aspect and seem to have largely reacted. This can be understood by the fact that tin increases the melt fluidity of Y123. Studies performed by Jee *et al.* [24] have effectively shown that a too fluid melt attacks the seed and tends to dissolve it. No single domain can then grow by epitaxy from it.

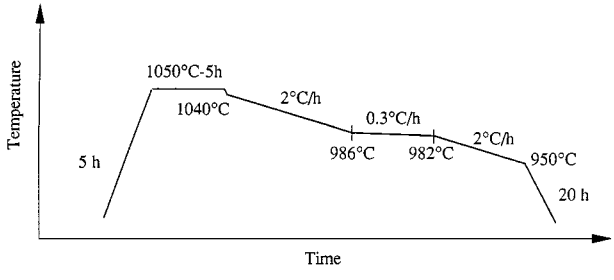

Figure 2 Thermal cycle defined for the texturation of cerium and tin doped samples (compositions B and C).

3.2. Characterisations

In order to observe the quality of the textured domains in the core of the pellets, samples of composition B were polished parallel to a (*ac*) or (*bc*) plane. The typical macrostructure is shown schematically in Fig. 4. Grains from homogeneous nucleation have significantly hindered the growth of the main domain, reducing his diameter in the vicinity of the pellet top surface (domain size 3 mm under the top surface $= 1.7 \times 1.7$ cm^2). The growth along the *c* axis has been stopped for the same reasons. The thickness of the monolith is 8 mm (total pellet thickness = 1.1 cm). Fine porosity can be observed inside the pellet, probably due to trapped CO_2 or O_2 gas. Thus, a "pre-sintering" step seems to be necessary to reduce porosity.

Microstructures of the samples have been observed using SEM. Figs 5a–c show the microstructures of composition A, B and C. Y211 particles size and morphology are similar for the 3 compositions and their diameter varies from 0.5 to 3 μm. Small precipitates appear when tin is added. No particular form can be associated with these inclusions and their size scarcely exceeds several hundreds of nanometers. As expected, their number is more significant in the 1 wt % doped sample. EDS analyses reveal that these compounds contain Y, Ba, Cu, Sn, Ce and O. Since the particle size is very small, no precise composition can be determined by this process. But by comparison between the analyses, we observe that the composition C inclusions contain more tin than composition B. This observation is consistent with Marinel *et al.* results [21]. They have identified a ϕ_2 phase, corresponding to $Ba_2(Y_{2/3-x}Cu_x)(Ce, Sn)_{4/3}O_y$ (this phase is close to the ϕ_1 phase, with formula $Ba_2Y_{2/3}(Sn_{4/3-x}Cu_x)O_{6-\delta}$, discovered by Delamare *et al.* [20] in tin doped YBCO). The more Sn they add initially, the higher the ratio Sn/Ce in the ϕ_2 particles. We precise that, although it exists similarities, the element contents are different in the phase we observe and the ϕ_2 phase. In particular, our compound appears to be far more rich in copper. TEM obervations and analyses to determine the exact composition are under investigation.

To investigate the influence of Sn + Ce doping on the superconducting properties, measurements of critical temperatures, current densities and levitation forces have been performed.

Critical temperatures of the three compositions A, B and C are illustrated on Fig. 6. The addition of tin shifts the T_c onset towards 92 K, which is closed to the critical temperature of pure YBCO. Transition widths are 2 K for A and C compositions and 0.5 K for the 0.25 wt% SnO_2 doped material.

Fig. 7 shows the critical current densities calculed from the magnetisation curves. Clearly, the best result is achieved in the 0.25 wt % SnO_2 doped sample. J_c reaches 9×10^4 A/cm^2 in self field, 5×10^4 A/cm^2 under 1 Tesla and 2.5×10^4 A/cm^2 under 2 T. These values correspond to the average of measurements performed on several cleaved pieces extracted from the same pellet. As the pieces come from different parts of the domain, the data vary in a small extent from one piece to another (maximum 15%). The highest critical current density obtained was 1×10^5 A/cm^2 in self field.

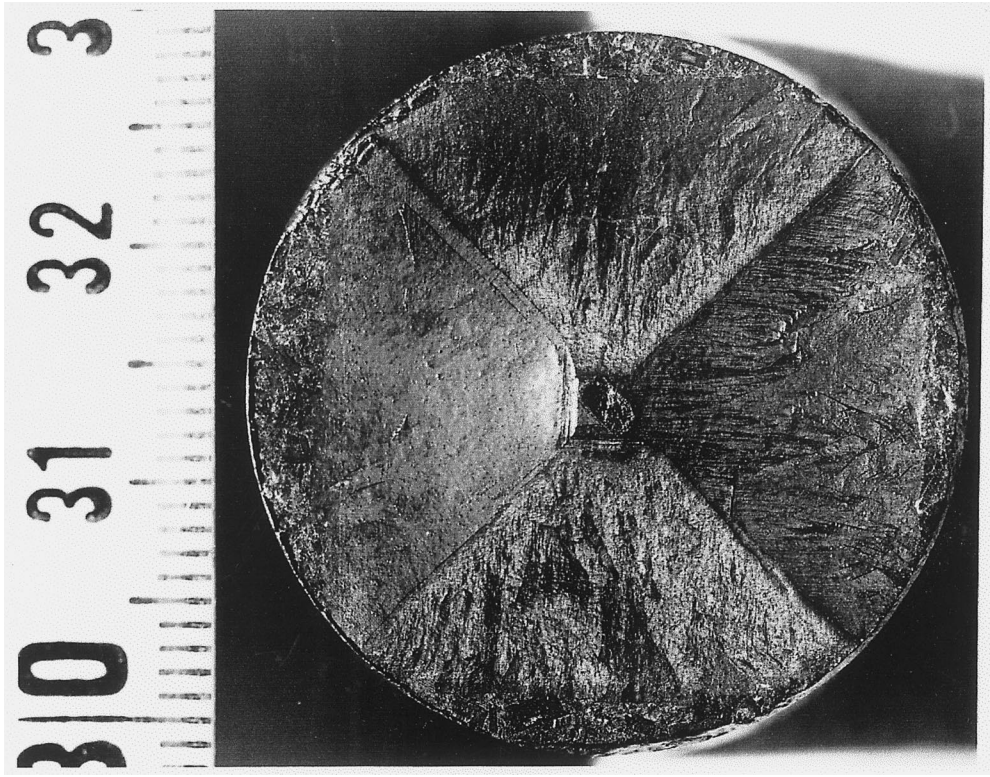

Figure 3 Photograph of a composition B pellet textured by the process defined in this article.

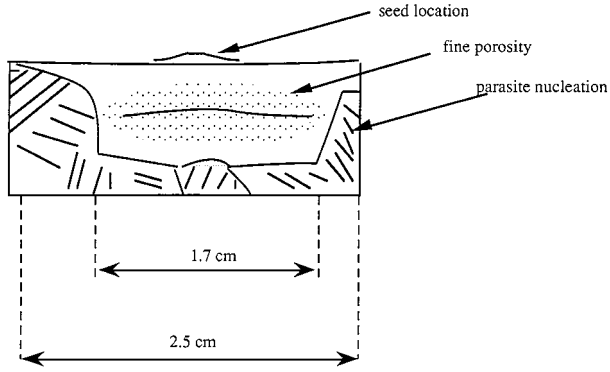

Figure 4 Drawing of the composition B pellet macrostructure parallel to the c direction. Homogeneous nucleation is important on the pellet sides and parasite grains have hindered the single domain growth.

To our knowledge, this is the highest value obtained in top seeded melt textured YBCO material. We want to underline that, as stated earlier, the texturing process is not yet optimised and yields non homogeneous material through the whole pellet. This explains the observed variations in J_c.

For what concerns the other compositions, the cerium doped sample exhibits 6.5×10^4 A/cm^2 in self field and 2×10^4 A/cm^2 under 1 Tesla; the 1 wt% SnO_2 (+0.5 wt% CeO_2) sample exhibits the lowest values with 4×10^4 A/cm^2 in self field and 7000 A/cm^2 under 1 Tesla. Thus, an optimum tin doping level may exist between 0.25 to 1 wt %.

Levitation forces of 2 equivalent sized monoliths of compositions A and B have been measured. Results are given in Table II. Nominal repulsive forces are similar for both compositions. No study has been performed on the C sample, since no large domain has been grown. To compare the samples effectively, forces should be reported per textured domain unit surface. Since the area of the Ce+Sn doped domain decreases quite rapidly with the distance to the top surface, this value is difficult to calculate. Field mappings will be more representative of the properties and are under way.

TABLE II Levitation forces measured on composition A and B pellets, in ZFC configuration, with a SmCo magnet ($Bs = 0.40$ T)

	Domain area	Levitation Force
Composition A	2.2×2.2 cm^2 (same value along *c*)	27 N
Composition B	2.5×2.5 cm^2 (1.7×1.7, 3 mm under the top surface)	28 N

4. Discussion

Doping elements have a significant influence on the decomposition temperature of YBCO. Ce reduces its value by 20 degrees. Earlier studies [25] have shown that Ce enters the Y123 matrix on the Y sites. We may assess that during the heating process, cerium reacts with Y123, resulting in a depression of $T_{\text{decomposition}}$. On the other hand, SnO_2 does not react with the Y123 matrix and thus does not modify $T_{\text{decomposition}}$. The combination of $CeO_2 + SnO_2$ appears to react with Y123 at a temperature, which is intermediate between the 2 dopants alone.

The addition of tin to the cerium doped samples has enhanced the growth rates. Indeed, as Sn increases the fluidity of the melt, the yttrium diffusion is improved and thus the yttrium supply at the growth fronts is greatly improved too. Growth rates in our case have

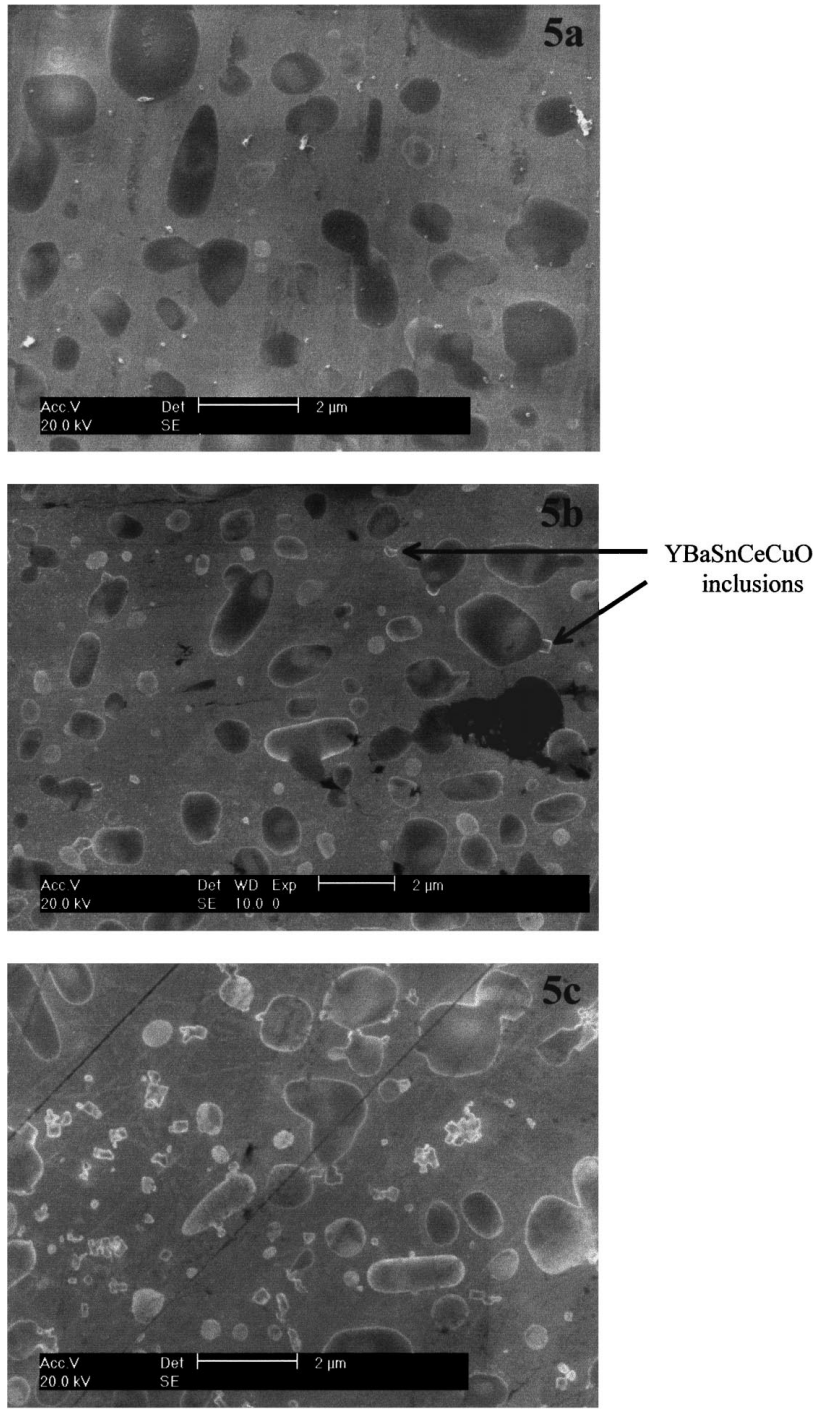

Figure 5 Microstructures of the different doped samples: (a) Composition A sample (cerium doped); (b) Composition B sample (cerium and tin doped); (c) Composition C sample (cerium and tin doped).

been multiplied by 4. The fact that our domain has been quite hindered by homogeneous grain nucleation is certainly due to a little underestimation of the bottom of the nucleation window combined with the significant growth rates of parasite domains, which are similarly accelerated. The improvement of the texture formation and bulk quality by the addition of a presintering step (homogeneity, decarbonatation, porosity) and by a slight shift of the nucleation window should be significant.

The T_c onset depression of cerium doped YBCO is now well known and attributed to cerium entering the Y123 matrix. Compositions B and C exhibit higher T_c onset, suggesting that tin prevents cerium from entering the matrix. In the liquid state, cerium, present in the melt, continues to act as an inhibitor of the Y211 coarsening. But during the peritectic recombination, tin rich inclusions seem to incorporate cerium. More tin is initially added, more inclusions are formed, more cerium is consumed and T_c onset is higher. Nevertheless, no clear explanation has been found regarding the variation of transition width.

Cerium doping leads to a homogeneous distribution of microsize Y211 particules in the textured material. Such small inclusions increase the flux pinning under low fields. Thus, the critical current densities of

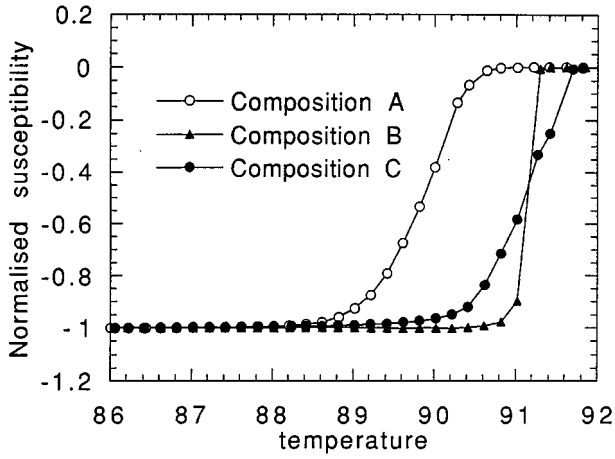

Figure 6 Normalised susceptibility of the different compositions versus temperature.

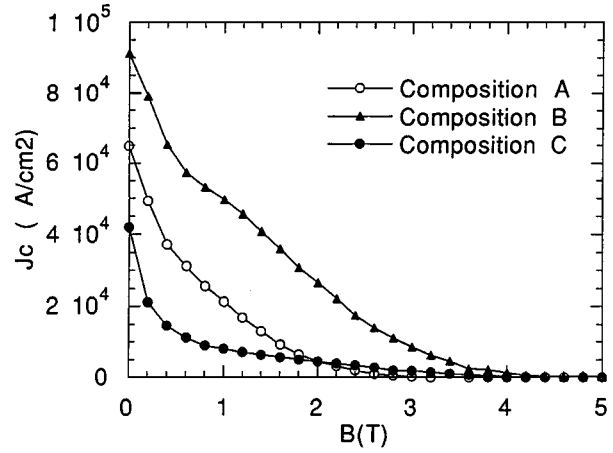

Figure 7 Critical current of the different compositions versus magnetic field.

compositions A and B reach high values in self field and very low fields. For composition B, two other factors contribute to the enhancement of J_c by comparison to cerium doped samples. First, T_c is increased by the addition of tin, and thus J_c at 77 K should be improved. Secondly, the submicron inclusions containing tin act as many additional pinning centers. In the case of 1 wt % SnO_2 doped sample, the decrease of J_c, although T_c increases, is attributed to the bad texture quality.

The important pinning under magnetic field of the composition B is more difficult to understand. The existence of small oxygen underdoped regions, around the tin particules for example, which could have explained such a behavior, is not consistent with a narrow transition of 0.5 K. Twin density may be increased by tin addition and TEM observations are required to study this effect further.

5. Conclusion

The effect of the doping with cerium and tin on YBCO top seeded melt textured pellets has been investigated. Although the texturing process and composition have not yet been really optimised, large pellets of $CeO_2 + SnO_2$ doped YBCO have been fabricated with composition 0.5 wt % $CeO_2 + 0.25$ wt % SnO_2. This doping mixture has shown to present the combined advantages of the two dopings alone : enhancement of the growth rates of Y123 thanks to tin, and fine Y211 trapped particles thanks to the action of CeO_2 in the melt. Moreover, the formation of a phase containing cerium and tin prevents the cerium from entering the Y123 matrix. This phase is dispersed in the form of submicron inclusions, that have a great influence on the pinning properties. Results obtained are quadrupled growth rates, shifted T_c towards 92 K with a transition width of 0.5 K and critical current densities as high as 9×10^4 A/cm^2 under self field, 5×10^4 A/cm^2 under 1 T and 2.5×10^4 A/cm^2 under 2 T. All these results make of the mixture 0.5 wt % $CeO_2 + 0.25$ wt % SnO_2 a very promising doping. Improvement of the texturing process, especially by the addition of a pre-sintering step, and study of optimal tin amount are under way. The composition of secondary phases and their role in the enhancement of superconducting properties are also under investigation.

References

1. H. FUJIMOTO, *JOM* (October 1998) 16.
2. R. ZENG, V. MURASHOV, T. P. BEALES, H. K. LIU and S. X. DOU, *Appl. Supercond.* **5** (1998) 201.
3. M. MURAKAMI, *Supercond. Sci. Technol.* **5** (1992) 185.
4. T. A. COOMBS, A. M. CAMPBELL, I. GANNEY, W. LO, T. TWARDOWSKI and B. DAWSON, *Mater. Sci. Eng.* **B53** (1998) 225.
5. C. K. Mc MICHAEL, K. B. MA, M. M. W. LIN, M. A. LAMB, R. L. MENG, Y. Y. XUE, P. H. HOR and W. K. CHU, *Appl. Phys. Lett.* **59** (1991) 2442.
6. S. NAGAYA *ISTEC J.* **10** (1997) 31.
7. V. CHAKRAPANI, D. BALKIN and P. Mc GINN, *Appl. Supercond.* **1** (1993) 71.
8. T. MEIGNAN and P. Mc GINN, *Supercond. Sci. Technol.* **10** (1997) 576.
9. J. C. L. CHOW, H. T. LEUNG, W. LO and D. A. CARDWELL, *ibid.* **11** (1998) 369.
10. J. WANG, I. MONOT, X. CHAUD, A. ERRAUD, S. MARINEL, J. PROVOST and G. DESGARDIN, *Physica C* **304** (1998) 191.
11. M. P. DELAMARE, I. MONOT, J. WANG and G. DESGARDIN, *J. Elec. Mater.* **24** (1995) 1739.
12. M. LEPROPRE, I. MONOT, M. P. DELAMARE, M. HERVIEU, CH. SIMON, J. PROVOST, G. DESGARDIN, B. RAVEAU, J. M. BARBUT, D. BOURGAULT and D. BRAITHWAITE, *Cryogenics* **34** (1994) 63.
13. P. Mc GINN, W. CHEN, N. ZHU, L. TAN, C. VARANASI and S. SENGUPTA, *Appl. Phys. Lett.* **59** (1991) 120.
14. I. MONOT, T. HIGUSHI, N. SAKAI and M. MURAKAMI, *Supercond. Sci. Technol.* **7** (1994) 783.
15. K. OSAMURA, N. MATSUKURA, Y. KUSUMOTO, S. OCHIAI, B. NI and T. MATSUSHITA, *Jap. J. Appl. Phys.* **29** (1990) L1621.
16. I. MONOT, K. VERBIST, M. HERVIEU, P. LAFFEZ, M. P. DELAMARE, J. WANG, G. DESGARDIN and G. VAN TENDELOO, *Physica C* **274** (1997) 253.
17. R. YU, J. MORA, N. VILALTA, F. SANDIUMENGE, V. GOMIS, S. PINOL and X. OBRADORS, *Supercond. Sci. Technol.* **10** (1997) 583.
18. Y.-S. LEE, H-.S. PARK, I.-H. KUK, G.-W. HONG and C.-J. KIM *Korean J. Mater. Res.* **8** (1998) 105.
19. C. LEBLOND, I. MONOT, J. PROVOST and G. DESGARDIN, *Physica C* **311** (1999) 211.
20. M. P. DELAMARE, PhD thesis, University of Caen, 1996.

21. S. MARINEL, I. MONOT, J. PROVOST and G. DESGARDIN, *Supercond. Sci. Technol.* **11** (1998) 563.
22. C. P. BEAN, *Rev. Mod. Phys.* **36** (1964) 31.
23. C. LEBLOND, I. MONOT, D. BOURGAULT and G. DESGARDIN, *Supercond. Sci. Technol.* **12** (1999) 405.
24. Y. A. JEE, G.-W. HONG, T.-H. SUNG and C.-J. KIM, *Physica C* **314** (1999) 211.
25. M. P. DELAMARE, M. HERVIEU, J. WANG, J. PROVOST, I. MONOT, K. VERBIST and G. VAN TENDELOO, *ibid.* **262** (1996) 220.

Received 13 July 1999
and accepted 11 April 2000